Water Science & Technology

Water Science & Technology Vol 90 No 7, 2070 doi: 10.2166/wst.2024.321

Utilization of waste hot air of medical oxygen plant in solar desalination unit employing jet impingement air heater for water production

Taranjeet Sachdev [a,*] and Aditya Thakur[b]

[a] Department of Mechanical Engineering, Shri Shankaracharya Institute of Professional Management and Technology Raipur, Raipur, CG, India
[b] Department of Mechanical Engineering, National Institute of Technology Raipur, Raipur, CG, India
*Corresponding author. E-mail: taranjeet84@gmail.com; t.sachdev@ssipmt.com

TS, 0000-0001-8196-6074

ABSTRACT

Many oxygen plants have been established specially during COVID-19 period and they are still serving for medical needs. The objective of the present work is to utilize solar and waste thermal energy of medical oxygen plants for water production. Humidification–dehumidification desalination (HDD) has been found suitable for this objective due to low temperature energy need during the process. The layout of an HDD unit has been presented to utilize waste heat, specially when solar energy is not much effective or absent. The system has been configured with a jet impingement solar air heater and a packed bed humidifier. A mathematical model has been developed and validated with the results of experiments. A comparative study of the proposed unit (HDD-O_2) and a conventional unit has been performed in terms of yield and gained output ratio (GOR). The optimum flow rates of working fluids found in the range 0.03–0.04 kg/s and the temperature of air and water resulted in a continuous gain in yield. The average yield and GOR of the HDD-O_2 unit were found to be 8.5 kg/d and 1.1 that could reach up to 11 kg/d and 1.4, respectively. The HDD-O_2 unit provided yield at the cost of 0.04 $/kg with a payback period of 1.73 years. The findings of the present work indicated the suitability of the HDD-O_2 plant for water production.

Key words: desalination, humidification–dehumidification, medical oxygen plant, renewable energy, solar thermal, waste heat

HIGHLIGHTS

- Novel arrangement of a desalination unit for using renewable (solar energy).
- Use of a medical oxygen plant for performance enhancement.
- Nocturnal yield can be achieved.
- Significant improvement in yield and gained output ratio.

GRAPHICAL ABSTRACT

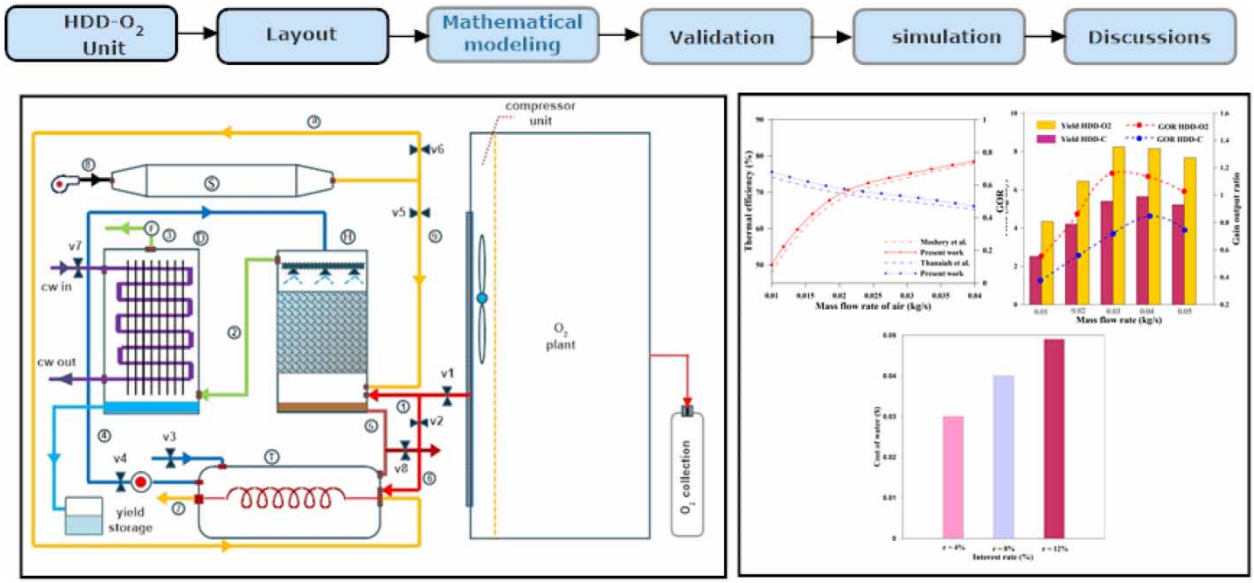

NOMENCLATURE

A_c	area of glass cover (m^2)
A_b	area of base plate (m^2)
A_j	heat transfer area of jet plate (m^2)
A_{pb}	back area of absorber plate (m^2)
C_g	specific heat of glass cover (J/kg K)
C_a	specific heat of air (J/kg K)
D_{h1}	hydraulic diameter of passage below jet plate (m)
D_{h2}	hydraulic diameter of passage above jet plate (m)
E	annual energy output
e	rib height (m)
h	heat transfer coefficient (W/m^2 K)
H	enthalpy (J/kg)
I	solar irradiance (W/m^2)
k	thermal conductivity (W/m K)
m_{a2}	mass of air in the passage below absorber (kg)
m_g	mass of glass cover (kg)
m_j	mass of jet plate (kg)
m_p	mass of absorber plate (kg)
M_a	mass flow rate of air (kg/s)
M_{fw}	mass flow rate of condensate water (kg/s)
M_w	mass flow rate of water (kg/s)
M_{mw}	mass flow rate of makeup water (kg/s)
Q	heat transfer term
Re	Reynolds number
T_{a2}	mean temperature of air below jet plate
T_{a2}	mean temperature of air below absorber plate
T_b	temperature of base plate
T_{fw}	temperature of condensate water
T_g	temperature of glass cover
T_j	temperature of jet plate
T_{mw}	temperature of makeup water
T_p	temperature of absorber plate
T_s	surrounding (ambient temperature)
T_{sky}	temperature of sky

T_w temperature of water
U_b bottom loss coefficient
V_w wind speed (m/s)
w specific humidity (kg/kg of dry air)
Z_1 height of upper channel (m)
α absorptivity
ε emissivity
τ time (s)
τ_g transmissivity of glass
η_p fin effectiveness
ψ average CO_2 emission by coal/annum
ϕ_{CO_2} annual CO_2 mitigation

INTRODUCTION

The importance of a medical oxygen plant in a medical facility is well evident because it provides life-saving oxygen. Many pressure-swing adsorption plants have been established for oxygen production, specially during the COVID-19 period, and those plants are still in operation for fulfilling O_2 requirements. These oxygen plants release hot air as waste from a compressor unit during their functioning period. The present work aims to utilize this hot air for potable water production through a humidification–dehumidification process. The simplicity of operation of the humidification–dehumidification desalination (HDD) process always appealed to researchers because of its utilization of low temperature thermal sources. However, in the case of sole solar assistance, effective production can be achieved over limited hours and this duration is not encouraging in moderate or cold climates.

Many configurations of an HDD unit have been developed by integrating low temperature thermal energy sources (Alghassab 2024) for heating process air, water, or both, which in due course, resulted in a higher yield. The augmentation of the humidification and dehumidification process has been proposed by Elminshawy *et al.* (2016) by utilizing geothermal energy with a solar HDD unit. The integrated unit provided the yield of 104 L/m^2 with an average gained output ratio (GOR) up to 1.58. Lawal *et al.* (2018) used a heat pump to fulfill the need of heating and cooling in the HDD system. The proposed integration with a heat pump resulted in increasing the GOR up to 8.8. Abdullah *et al.* (2018) proposed a hybrid unit by integrating an HDD process with a wick-type solar still. The effect of the packing material used in the humidifier was studied and a GOR of 5.4 was found. Shojaei *et al.* (2020) integrated a solar humidifier in an HDD unit which was also configured with a heat pump. The results of these experiments revealed a maximum yield of 1 kg/h and a GOR of 2.36.

Chen *et al.* (2020) combined an HDD unit with an evaporative air-cooling unit to achieve thermal comfort and yield simultaneously. The proposed combination resulted in 25–125 L/h water and a GOR in the range 1.6–2.5. Qasem *et al.* (2020) coupled an HDD unit with an absorption refrigeration unit for water production in large quantities. A yield rate of 1.145 L/h was obtained by the proposed configuration with a GOR of 4.54. Jabari *et al.* (2020) used a solar Stirling engine for power and heat generation. It also ran an HDD system for water production. Sachdev *et al.* (2020) proposed to couple an HDD unit with a wind tower for simultaneous production of water and thermal comfort. The proposed configuration resulted in 4.5–5 kg yield per day. Kabeel *et al.* (2022) utilized cold air of an HDD unit for enhancing the performance of the air-conditioner. The proposed unit resulted in a daily yield of 36.49 L and an approximate 60.9% rise in the GOR.

Alrbai *et al.* (2022) utilized a fogging nozzle for augmenting the humidification process in an HDD unit which resulted in a maximum GOR of 3.4. Santosh *et al.* (2022) performed experiments on an HDD unit having an energy supply from waste heat at a temperature range of 45–70°C. The maximum yield of 1.398 mL/h was found due to the proposed modifications. Khass *et al.* (2022) analyzed an HDD system with multi stage humidification and a 151.2 kg/h yield was reported with a GOR of 1.995. Abdel Dayem & Al Zahrani (2022) studied the effect of packing materials in humidification by using a wet cooling tower as the humidifier. The study reported a GOR of 4.3 and a yield of 25 L/d. Welepe *et al.* (2022) presented a humidifying collector for minimizing the amount of liquid and used it with an HDD unit. The performance of the proposed system was improved by 1.3–32.2 times compared to a conventional system and a yield of 2.923 kg/h was reported.

Shaikh & Ismail (2023) utilized a multistage dehumidifier to reduce the condensing area and cost. The proposed configuration augmented the yield by 6.24% and the output ratio improved by 6.75%. Shamet *et al.* (2023) utilized heat of a diesel generator which was otherwise released as waste. The analysis of four different configurations of an HDD unit resulted in a maximum GOR of 3.2. Abedi *et al.* (2023) proposed to use a solar chimney with an HDD system which can provide

600 L of water per day. Easa *et al.* (2023) examined a high-speed rotary humidifier in an HDD unit. The maximum yield of about 17 kg was obtained at slot bore and spray speed of 0.001 m and 1,200 rpm, respectively. Zarei & Adibi (2023) used rushing packing in the humidifier of the HDD unit and achieved a daily yield of 312 L.

It is clear from the available literature that numerous configurations of HDD units have been developed for the augmentation of yield. In continuation, the present work proposes a layout of the HDD unit for utilizing waste hot air of medical O_2 plants. This is a novel approach as (i) waste heat of medical O_2 plants has not been utilized in HDD systems so far; (ii) in contrast to conventional solar HDD units, this approach enables the unit for nocturnal yield (or duration when solar energy is ineffective); (iii) the proposed system is configured with a solar air heater having jet plate (SAHJP) with novel ribs and a packed bed humidifier; and (iv) transient behavior of the system was analyzed. Additionally, a moderate climate (Raipur, India) was used for performance evaluation instead of a favorable hot summer climate. For comparative analysis of the proposed unit (HDD-O_2) with a conventional (HDD-C) unit, a mathematical model was developed and validated with the available experimental results. Performance parameters such as yield, GOR, humidifier dimensionless parameters, etc. have been evaluated with the help of a computer simulation program for variable inputs. Finally, economic competitiveness of the proposed system was also assessed.

MATERIALS AND METHODS

System configuration and description

The functioning of the proposed plant depends on the different situations of availability of hot air from O_2 plants, SAHJP, or both. In the first situation, hot air is available from an O_2 plant but an air heater is not operational or very much effective. This situation may represent nocturnal hours, morning or evening hours when solar energy is either absent or not effective for air heating. In the absence of hot air from the SAHJP, O_2 plants can be scheduled to operate and yield can be produced in an HDD unit by consuming waste hot air of O_2 plants. In this manner, additional duration of water production can be achieved at night and late evening/early morning, which is a distinct feature of the proposed unit (named as HDD-O_2 for further discussions) over conventional solar HDD units. The schematic outline of the proposed HDD-O_2 system for utilizing waste hot air of medical oxygen plants in potable water production is depicted in Figure 1 and a description of the system components are listed in Table 1.

In the proposed system, hot air coming from O_2 plants was divided into two routes to incorporate the additional advantage of water heating. In the first route 1-2-3, air follows the states to the humidifier and the dehumidifier for water production, while the second route 6-7 serves to preheat water before supplying to the humidifier. The flow of hot air in route 6-7 depends on the availability of hot air on the basis of the size or number of O_2 plants. At the same time, feed water from the storage tank follows the state 4-5 through the humidifier. Valves v1 and v2 regulate the flow of air and v4 ensures the necessary water flow in the humidifier through a pump. The brine at state 5 can be regulated by v8 for recirculating in the process or releasing out. A fan was also provided at the outlet of the dehumidifier for maintaining the proper flow of air in the system. The feed water availability and salinity can be ensured by attachments provided for supplying makeup water and removing the brine.

In the second situation of functioning, hot air is available from the SAHJP and the O_2 plant is not operational. This situation may represent the limited diurnal hours of a day when solar thermal energy is effectively available for heating ambient air. The O_2 plants can operate in any hours of the day as per the need; however, for water production, it is beneficial if the O_2 plants are scheduled to operate during the hours of ineffective solar energy. In this situation, the system follows a conventional process of humidification and dehumidification, and is named as HDD-C for further discussion. Here, ambient air follows the states 8-9-2-3 for yield formation and water from the storage tank follows the state 4-5. In this mode of operation, valve v5 regulates the flow of air coming from the SAHJP and valve v6 will be completely closed to avoid any diversion of air. Valves v1 and v2 will also be closed as the O_2 plant is inoperative, and thus, it does not supply hot air. A blower was provided so that ambient air can be supplied to the SAHJP for heating. Similar to HDD-O_2, brine recirculation can be regulated in HDD-C by v8.

In the third situation of operation, hot air from both O_2 plants and air SAHJP is available; however, hot air from the SAHJP will augment the performance of the proposed unit through humidification–dehumidification when its temperature is higher than the temperature of air coming from the O_2 plants. This situation may occur for a very limited number of hours, depending on the location when solar thermal energy is at its peak, and this duration will be minimum in moderate or cold climates. In these hours, air from the SAHJP will enter the humidifier for following the HDD process while hot air from the O_2 plants

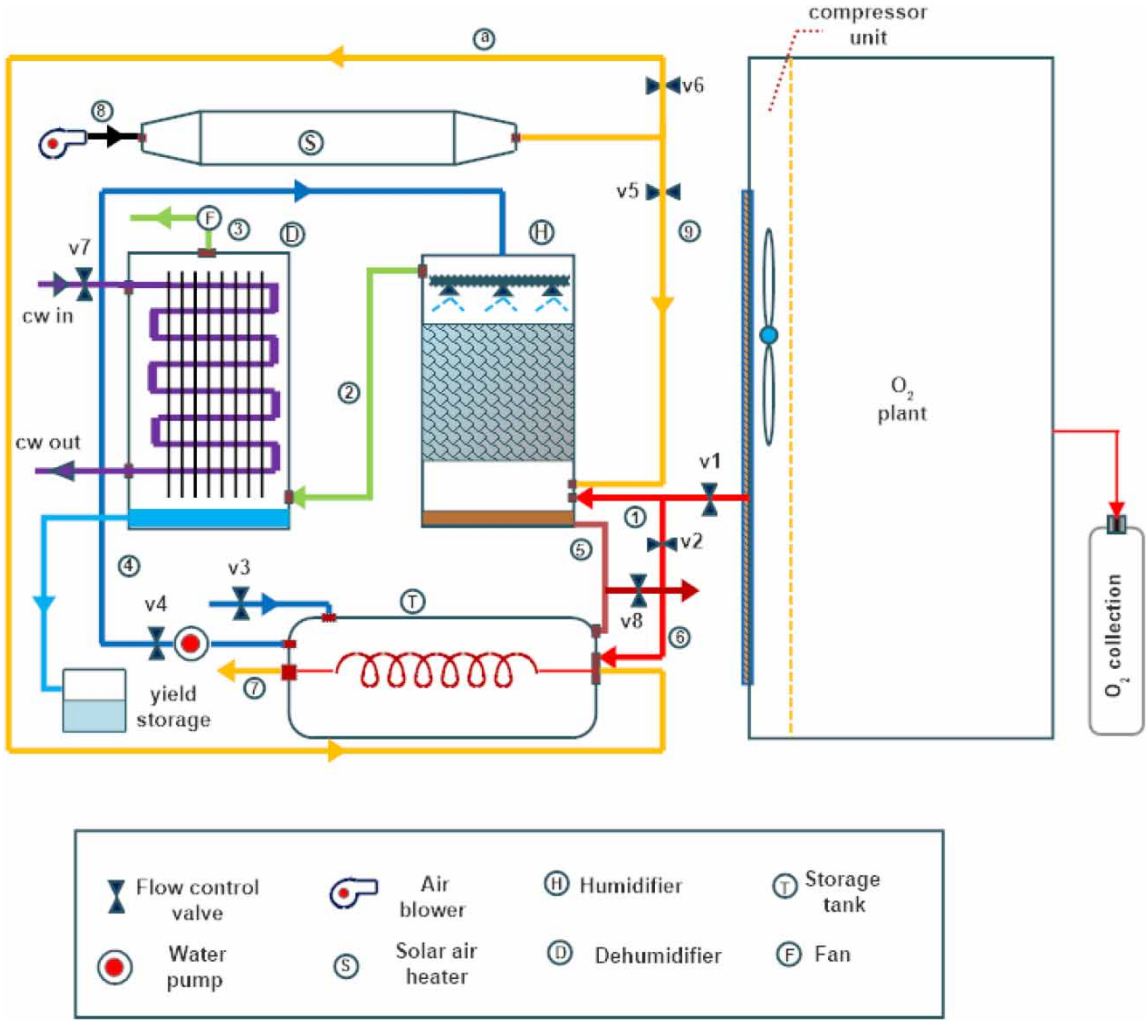

Figure 1 | Schematic of a desalination unit.

Table 1 | Components of the proposed system

Component	Type	Specification
Air heater	Solar-jet impingement	1.4 × 0.7 m
Humidifier	Packed bed	Dimension (80 × 40 × 40 cm)
Dehumidifier	Finned tube	Dimension (70 × 40 × 40 cm)
Storage tank	Water tank with tubes for hot air flow	Capacity (400 L)
Fan	Electric	Size and power (20 cm, 30 W)
Pump	Electric water pump	Max flow and power (15 L/min, 40 W)

will serve to preheat the feed water in the storage tank. In the remaining hours, when the temperature of air supplied by the O_2 plants is higher, valves v5 and v6 will be closed to avoid any mixing with lower temperature air of the SAHJP; otherwise, moisture carrying capacity (as it depends on air temperature) of air will be affected. Thus, the system will again start to operate as in the first situation described previously. As the system mostly follows the first or second situation, except in the few hours of peak solar energy, the performance under the third situation has not been evaluated in this work.

On the basis of the situations explained, the present work compares the performance of HDD-C and HDD-O_2. The difference of these two can be summarized as operational hours of the HDD-C unit depends on the availability of effective solar energy, whereas HDD-O_2 can operate for additional hours by consuming hot air of the O_2 plants in the absence of solar irradiance. The various states followed by process air in HDD-O_2 and HDD-C units are illustrated in Figure 2.

Mathematical modeling

The operation of HDD-O_2 and HDD-C was explained with the help of Figure 1 in the previous section. In the present section, energy/mass balance has been considered for HDD-O_2/HDD-C components to develop a mathematical model for transient behavior. The schematic of a solar air heater with jet impingement used with the HDD process is illustrated in Figure 3 and Equations (1)–(6) are the corresponding governing equations. The mathematical model suggested by Matheswaran *et al.*

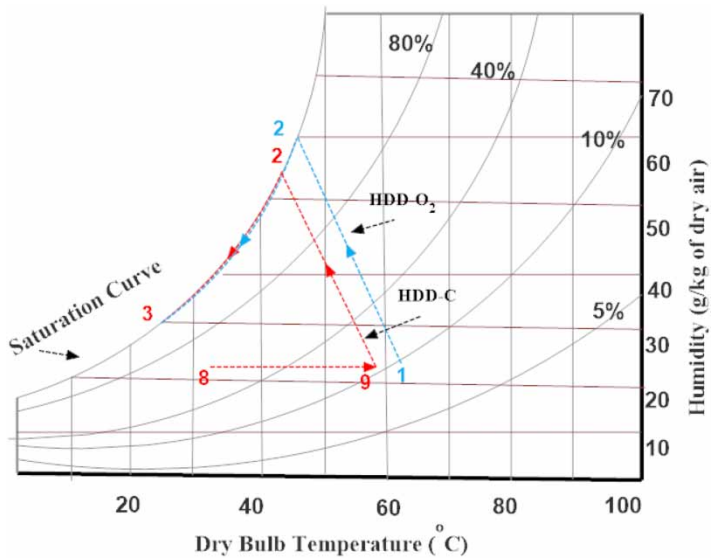

Figure 2 | States of air in HDD-O_2 and HDD-C.

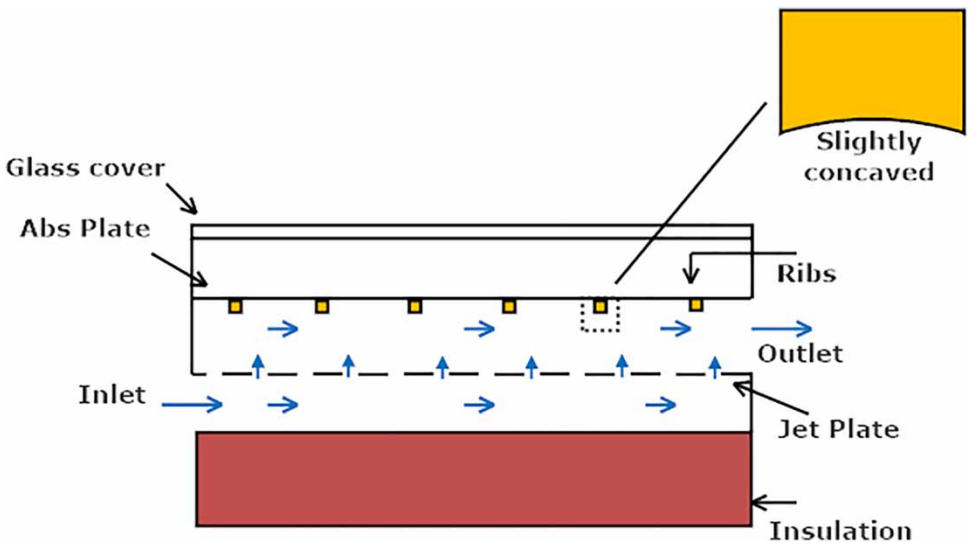

Figure 3 | Jet impingement solar air heater.

(2018) was followed for the development of these equations; however, the suggested model has been modified as per the design and operation of the present work, i.e. transient behavior and concaved ribs.

The glass cover receives solar energy and, simultaneously, interacts with the ambient and absorber plates placed at the bottom. Consequently, the energy balance is

$$\frac{dT_g}{d\tau} = \left(\frac{1}{m_g C_g}\right)\{I\alpha_g A_C + Q_{g/p(R)} - Q_{g/s(C)} - Q_{g/\mathrm{sky}(R)} + Q_{g/p(C)}\} \tag{1}$$

The absorber plate receives solar irradiations transmitting through the glass cover. Additionally, it interacts with air flowing beneath the jet plate. Therefore,

$$\frac{dT_p}{d\tau} = \left(\frac{1}{m_p C_p}\right)\{I\alpha_g \tau_g A_c - Q_{g/p(c)} - Q_{g/p(R)} - Q_{p/a2(C)} - Q_{p/j(r)}\} \tag{2}$$

The air coming through the jet plate impinges on the bottom surface of the absorber plate and, while flowing through the air channel, heat interaction takes place with the absorber and jet plates:

$$\frac{dT_{a2}}{d\tau} = \left(\frac{1}{m_{a2} C_{a2}}\right)\{Q_{p/a2(C)} + Q_{a2/j(c)} - M_{a2} C_{a2}(T_{a2o} - T_{a2i})\} \tag{3}$$

The jet plate is in contact with air on both sides and, additionally, heat interaction takes place with the absorber plate and the base plate; so, for energy balance,

$$\frac{dT_j}{d\tau} = \left(\frac{1}{m_j C_j}\right)\{Q_{p/j(R)} + Q_{j/a2(C)} - Q_{j/a1(C)} - Q_{\mathrm{plate}/gi(R)} - Q_{j/b(R)}\} \tag{4}$$

The air flowing below the jet plate interacts with the jet plate and the base plate to gain temperature; consequently,

$$\frac{dT_{a1}}{d\tau} = \left(\frac{1}{m_{a1} C_{a2}}\right)\{Q_{j/a1(C)} + Q_{b/a1(c)} - M_{a1} C_{a1}(T_{a1o} - T_{a1i})\} \tag{5}$$

The base plate is the last component to be considered in the mathematical model of this air heater. The energy balance is

$$\frac{dT_b}{d\tau} = \left(\frac{1}{m_b C_b}\right)\{Q_{j/b(R)} - Q_{b/a1(C)} - Q_{b/s}\} \tag{6}$$

The hot process air coming either from the O_2 plants or the air heater absorbs moisture in the humidifier and, finally, moisture condenses into yield in the dehumidifier. Equations (7) and (8) deal with energy/mass interactions during humidification whereas Equations (9) and (10) correspond to the dehumidifier:

$$M_{\mathrm{a\_hi}}\,(H_{\mathrm{a\_ho}} - H_{\mathrm{a\_hi}}) = M_{\mathrm{w\_hi}} C_w T_{\mathrm{w\_hi}} - M_{\mathrm{w\_ho}} C_w T_{\mathrm{w\_ho}}, \tag{7}$$

$$M_{\mathrm{w\_ho}} + M_{\mathrm{a\_ho}} w_{\mathrm{h\_o}} = M_{\mathrm{w\_hi}} + M_{\mathrm{a\_hi}} w_{\mathrm{h\_i}} \tag{8}$$

The proposed system can operate in two approaches named as HDD-O_2 and HDD-C. In the case of HDD-O_2, air coming from a medical O_2 unit enters the humidifier, whereas for HDD-C, air from the outlet of the air heater enters the humidifier. Therefore, temperature and specific humidity values at the inlet of the humidifier can be taken as per the approach of operation. The mass flow rate of air will be constant because there is no leakage of air from the humidifier:

$$M_a.\,(H_{\mathrm{a\_di}} - H_{\mathrm{a\_do}}) = M_{\mathrm{w\_di}} C_w (T_{\mathrm{w\_do}} - T_{\mathrm{w\_di}}) + M_{\mathrm{fw}} C_w T_{\mathrm{fw}}, \tag{9}$$

$$M_{\mathrm{fw}} = M_a(W_3 - W_4) \tag{10}$$

Energy balance equation for the storage tank is

$$m_{w\_t}.\ C_w \frac{dT_{wt}}{d\tau} = M_{w\_to}C_wT_{w\_to} + M_{mw}C_wT_{mw} - M_{w\_ti}C_wT_{w\_ti} + Q_{gain} - Q_{loss} \tag{11}$$

An important performance parameter for HDD is the GOR, which correlates the energy needed for yield and energy input. This parameter can be calculated as (Thanaiah *et al.* 2021)

$$\text{GOR} = \frac{M_{fw}\ .\ h_{fg}}{Q_{in}} \tag{12}$$

The mass transfer that took place in the humidifier can be expressed as (Thanaiah *et al.* 2021)

$$\frac{m_a}{m_w}\ (h_{a_{ho}} - h_{a_{hi}}) = \frac{kaV}{m_w}\left\{\frac{(h_{w\_hi} - h_{a_{ho}}) - (h_{w\_ho} - h_{a\_ho})}{\ln\dfrac{(h_{w\_hi} - h_{a\_ho})}{(h_{w\_ho} - h_{a\_ho})}}\right\} \tag{13}$$

Various correlations for calculating the heat transfer terms and thermophysical properties of process air are listed in Table 2.

RESULTS AND DISCUSSION

The mathematical model presented in the previous section was solved in MATLAB for performance comparison of HDD-O_2 and HDD-C. The ordinary differential equations available in the transport model of SAHJP were solved using the fourth-order Runge–Kutta method for air outlet temperature. Thereafter, results were used as input for the calculation of performance parameters with the help of governing equations related to the humidifier, dehumidifier, and storage tank. The ambient conditions involved are represented in Figure 4 and the parameters used for simulations are listed in Table 3.

Validation of model

First of all, the simulation code developed for performance comparison of HDD-O_2 and HDD-C has been validated to ensure the accuracy of results. The experimental results of Moshery *et al.* (2021) and Thanaiah *et al.* (2021) are used for validating the mathematical model in terms of thermal efficiency (air heater) and GOR (HDD system). The comparison between experimental and simulated results with identical operating and design parameters are depicted in Figure 5. It is evident from the comparison that mean deviation is below 5%, and thus, good agreement of the results is ensured.

Figure 6 shows the hourly variation in air temperature at the outlet of the SAHJP for the considered ambient condition. It is clear that the air temperature before 11 am and after 4 pm is considerably low and, therefore, cannot contribute very much for water production. As discussed earlier, HDD-O_2 can play its role by utilizing waste heat of O_2 plants for achieving additional yield compared to HDD-C. In performance comparison, the production run of HDD-C is from 11 am to 4 pm, whereas HDD-O_2 additionally runs from 8 am to 11 am and 4 pm to 7 pm.

The variation in yield and GOR of HDD-O_2 and HDD-C are depicted in Figure 7. Figure 7(a) shows the variation of yield and GOR with the mass flow rate of air at the inlet of the humidifier for both HDD-O_2 and HDD-C. It is evident that an increase in the air flow rate in the range of 0.03–0.04 kg/s enables the systems to achieve a higher GOR, whereas with a further rise in the air flow rate, a slight dropping trend in output was observed.

The reason for this can be explained with yield variations, which is the highest in the air flow range of 0.03–0.04 kg/s. An approximate 91% improvement in the GOR of HDD-O_2 and 120% improvement in the GOR of HDD-C was found. HDD-O_2 resulted in 53.1% higher GOR in comparison to HDD-C when the air flow rate was increased to the 0.03–0.04 kg/s range, and overall, HDD-O_2 resulted in about 50.2% higher GOR. The increase in the mass flow rate of air initially allowed to carry higher quantity of moisture which ultimately turns to higher yield. Therefore, the GOR was also found to increase but a further higher rate does not contribute very much in favor of the GOR.

Table 2 | (a) Equations involved in the mathematical model related to heat transfer and (b) equations of the thermal properties of air (Yamali & Solmus 2006)

S.N.	Heat transfer term	Equation
(a)		
1	$Q_{g/p\ (R)}$	$A_c h_{g/p\ (R)}(T_p - T_g)$
2	$Q_{g/s(C)}$	$A_c h_{g/s\ (C)}(T_g - T_s)$
3	$Q_{g/\mathrm{sky}(R)}$	$A_C\ h_{g/\mathrm{sky}}\ (T_g - T_{\mathrm{sky}})$
4	$Q_{g/p(C)}$	$h_{g/p(C)}(T_p - h_g)\ A_c$
5	$Q_{p/a2(C)}$	$h_{p/a2(C)}(T_p - T_{a2})\ A_{pb}\eta_p$
6	$Q_{p/j(R)}$	$h_{p/j(R)}(T_p - T_j)\ A_{pb}$
7	$Q_{a2/j(C)}$	$h_{j/a2(C)}(T_j - T_{a2})\ A_j$
8	$Q_{j/a1(C)}$	$h_{j/a1(C)}(T_j - T_{a1})\ A_j$
9	$Q_{j/b(R)}$	$h_{j/b(R)}(T_j - T_b)\ A_j$
10	$Q_{b/a1(C)}$	$h_{b/a1(C)}(T_b - T_{a1})\ A_b$
11	$Q_{b/s}$	$U_b(T_b - T_s)\ A_b$
	H.T.C	**Equation**
12	$h_{\mathrm{g/p\ (R)}}$	$\sigma(T_g^2 + T_p^2)\ (T_g + T_p)/\frac{1}{\varepsilon_g} + \frac{1}{\varepsilon_p} - 1$
13	$h_{g/s(C)}$	$2.8 + 3\mathrm{V}_w$
14	$h_{\mathrm{g/sky(R)}}$	$\varepsilon_{\mathrm{g}}\sigma(T_g^2 + T_{sky}^2)\ (T_g + T_{sky})$
15	$h_{g/p(C)}$	$\left(\frac{k}{Z_1}\right)[1 + 1.44\left\{1 - \frac{1708\ (Sin\ 1.8)^{1.6}}{R_a.\ \cos\emptyset}\right\}\left\{1 - \frac{1708}{R_a.\ \cos\emptyset}\right\}^{+} + \left\{\left(\frac{R_a\cos\emptyset}{5830}\right)^{1/3} - 1\right\}^{+}$
16	$h_{p/a2(C)}$	$\left(\frac{k}{D_{h2}}\right)\{0.001047\ Re^{1.3186}(\frac{e}{D_{h2}})^{0.3772}\}$
17	$h_{\mathrm{p/j\ (R)}}$	$\sigma(\mathrm{T}_p^2 + \mathrm{T}_j^2)\ (\mathrm{T}_p + \mathrm{T}_j)/\frac{1}{\varepsilon_p} + \frac{1}{\varepsilon_j} - 1$
18	$h_{j/a2(C)}$	$(0.0293Re2^{0.8})\left(\frac{K}{D_{h2}}\right)$
19	$h_{j/a1(C)}$	$(0.0293Re1^{0.8})\left(\frac{K}{D_{h1}}\right)$
20	$h_{\frac{\mathrm{j}}{\mathrm{b}}(\mathrm{R})}$	$\sigma(\mathrm{T}_j^2 + \mathrm{T}_b^2)\ (\mathrm{T}_j + \mathrm{T}_b)/\frac{1}{\varepsilon_b} + \frac{1}{\varepsilon_b} - 1$
21	$h_{b/a1(C)}$	$(0.0293Re1^{0.8})\left(\frac{K}{D_{h1}}\right)$
(b)		
Property	**Equation**	
Thermal conductivity (k)	$0.0244 + 0.6773 \times 10^{-4}T$	
Thermal diffusivity (α)	$7.7255 \times 10^{-10} \times T^{1.83}$	
Kinematic viscosity (υ)	$0.1284 \times 10^{-4} + 0.00105\ \times\ 10^{-4}T$	
Enthalpy (h)	$2.82 \times 10^{-5}T^4 - 0.00106T^3 + 0.0615T^2 + 1.32\,T + 10.5$	
Specific humidity (w)	$7.7 \times 10^{-7}T^3 - 1.9510^{-5}T^2 + 0.00071\,T + 0.02$	

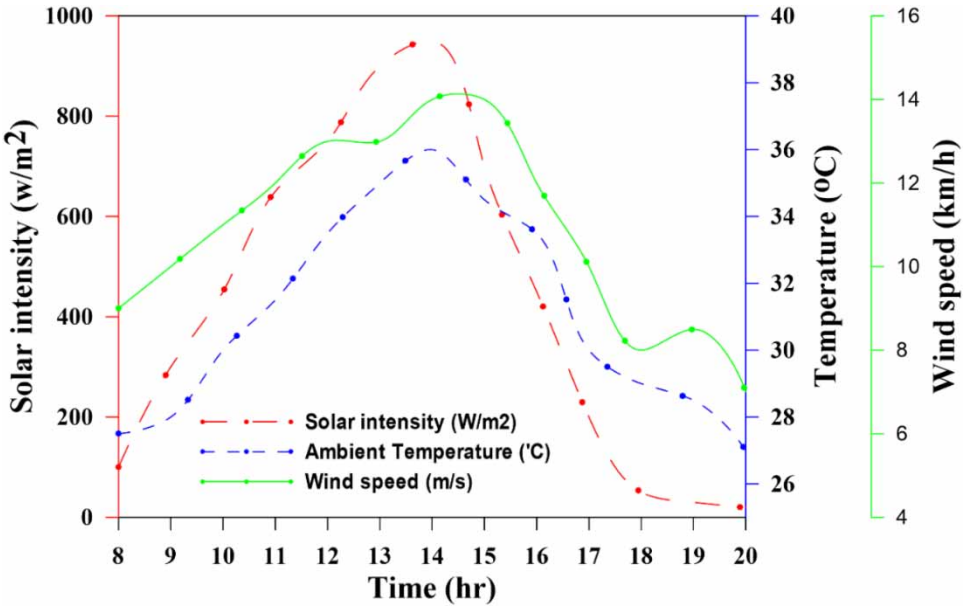

Figure 4 | Ambient data used in simulation.

Table 3 | Parameters used for simulation

Parameter	Value
Location	21.2514° N, 81.6296° E Raipur (India)
Collector dimension	1.4 × 0.3 m
Depth of upper channel	0.03 m
Depth of lower channel	0.04 m
Thickness of insulation	0.05 m
Thermal conductivity of insulation	0.032(W/mK)
Absorptivity of absorber plate	0.9
Transmissivity of glass cover	0.9
Emissivity of glass cover	0.9
Emissivity of absorber plate	0.9
Emissivity of jet plate	0.9
Streamwise pitch ratio	0.043
Spanwise pitch	0.435
Jet diameter ratio	0.435
Rib dimension	0.003 × 0.003 m
Pitch	0.01 – 0.04 m
Air mass flow rate	0.025 kg/s
Water mass flow rate	0.025 kg/s
Water mass flow rate in dehumidifier	0.03 kg/s
Mass of absorber plate	4.5 kg
Mass of base plate	4.5 kg
Mass of glass	3.5 kg
Glass emissivity	0.9
Storage tank	400 L
Temperature of air from O_2 plant	65°C

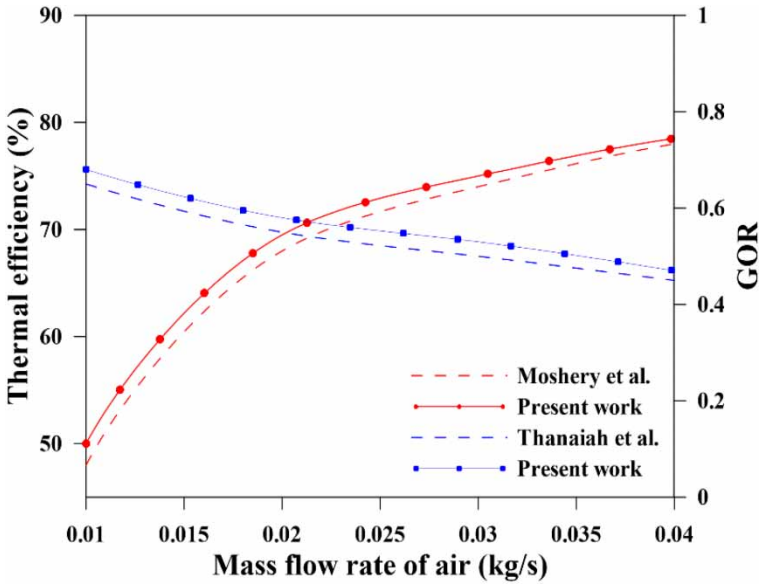

Figure 5 | Validation of the present work.

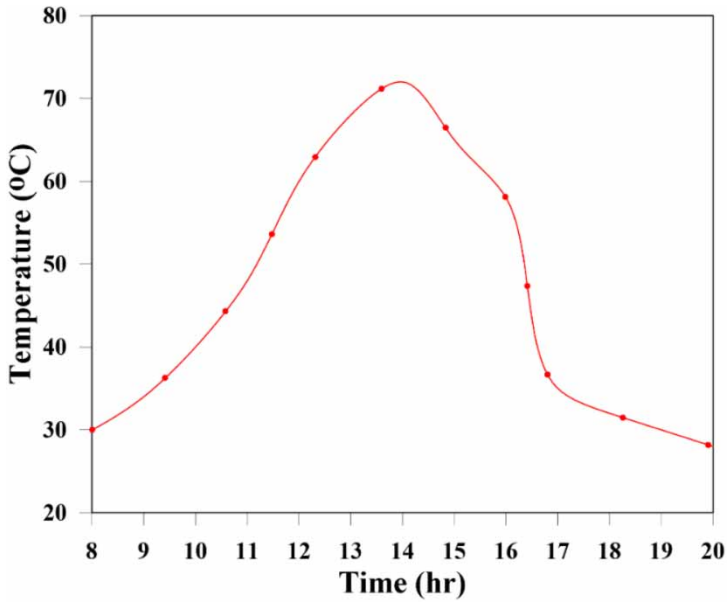

Figure 6 | Air outlet temperature of the SAHJP.

Figure 7(b) illustrates the variation in the GOR and yield of HDD-O_2 and HDD-C systems with water temperature fed to the humidifier. It is clear that with an increase in water temperature, the GOR also increased continuously. For the considered temperature range, the GOR of HDD-O_2 increased by 20.6% and this gain for HDD-C is 18.2%. At the same time, the GOR of HDD-O_2 is about 29% higher than the GOR of HDD-C at 45°C whereas, on average, it is 17% more in the considered temperature range. Due to the dependency of the GOR on yield, this variation is very similar to that of yield. The HDD-O_2 system resulted in about 49% higher yield than HDD-C. This behavior is evident as air interacting with water at higher temperatures itself gains temperature, which also increases the moisture carrying capacity of air. The air carrying more moisture can provide a higher yield and, therefore, an improvement in the GOR was achieved.

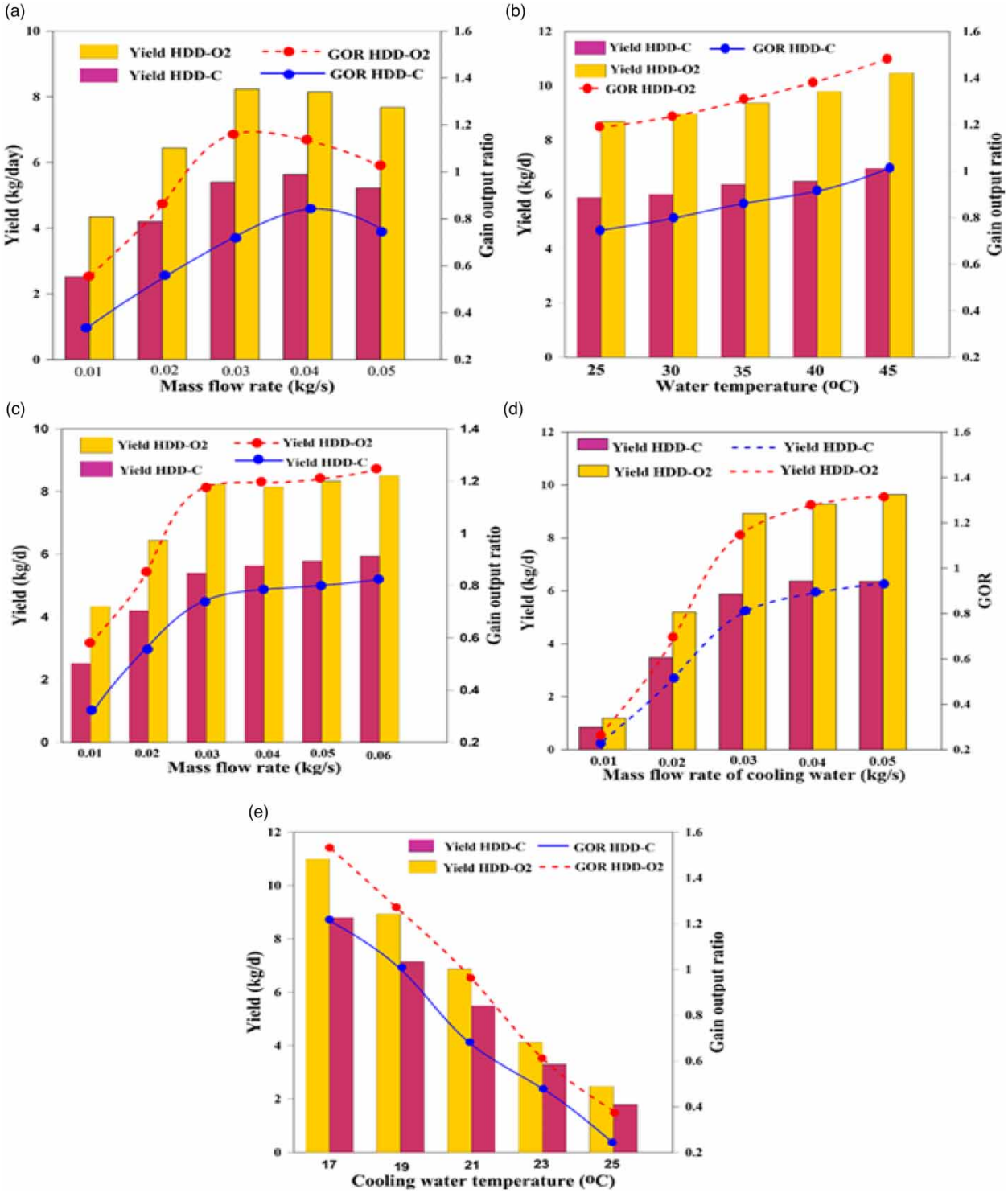

Figure 7 | Variation of yield/GOR of HDD-O_2 and HDD-c.

Figure 7(c) reveals the dependency of yield and GOR with the mass flow rate of feed input to the humidifier. A swift gain in the yield of HDD-O_2 and HDD-C can be observed till a mass flow rate of 0.03 kg/s, which is 95 and 83%, respectively. Thereafter, an increase in feed was found to be marginally beneficial in augmenting the yield as only about 5% gain was found for

HDD-O_2 and HDD-C. On an overall basis, HDD-O_2 resulted in about 48% higher yield compared to HDD-C. This increase in yield was also responsible for the thermal energy utilized for water production and, therefore, led to an increase in the GOR in a very similar manner. The increase in GOR for HDD-O_2 was about 98% and the same for HDD-C was about 88% over the considered flow rate of 0.01–0.06 kg/s. The observed behavior is related to the amount of moisture available in process air, which increased rapidly with the amount of feed water available up to 0.03 kg/s. Since air at particular temperatures has limited moisture carrying capacity, further available feed cannot contribute very much in increasing moisture, and this is evident after the flow rate of 0.03 kg/s.

The effect of supplying more amounts of cooling water in HDD-C and HDD-O_2 for dehumidification is illustrated in Figure 7(d). It is clear that both yield and GOR upsurge with the rate of cooling water. However, this increase is mainly up to a flow rate of 0.035 kg/s as the yield of HDD-O_2 increased about 400% up to this flow rate. Thereafter, with further increase in the flow rate up to 0.05 kg/s, only 7% improvement was observed. Due to the dependency of the GOR on yield, it also followed a very similar variation. The GOR of HDD-O_2 was found to be about 53% (on average) higher in comparison to that of HDD-C. The results made clear that higher amounts of cooling water augmented the yield and GOR by carrying the heat of condensation. Figure 7(e) depicts the variation of yield and GOR with the temperature of cooling water supplied for condensing water vapor. Both the performance parameters were found to have higher values with lower temperature of water as lower temperature augments the heat transfer associated with condensation. On average, the yield of HDD-O_2 was found to be 37% higher over HDD-C for the considered temperature variation between 17 and 25°C and, at the same time, this improvement was 25% for the GOR.

The variation of the dimensionless parameter (kav/M_w) of the humidifier with mass flow ratio and water temperature is shown in Figure 8. The considered humidifier parameter continuously decreased with an increase in the mass flow ratio and this reduction was about 54% as the mass flow ratio increased in the range 1–3. At the same time, the relation between the humidifier parameter and the temperature of feed water is also depicted in Figure 8 where the humidifier parameter was found to increase with temperature. This increase was about 60% when the water temperature varied from 25 to 50°C.

Economic analysis

The cost competitiveness of the HDD-O_2 unit has been evaluated for three different interest rates with the help of methodology followed by Faizan *et al.* (2022) and Sun *et al.* (2022). The summary of analysis is provided in Table 4 which is segmented into three parts. Part (a) deals with the calculation of capital cost by considering the cost of individual components (as per local market), part (b) lists the assumed parameters, and finally, part (c) lists the equations used for analysis. The result

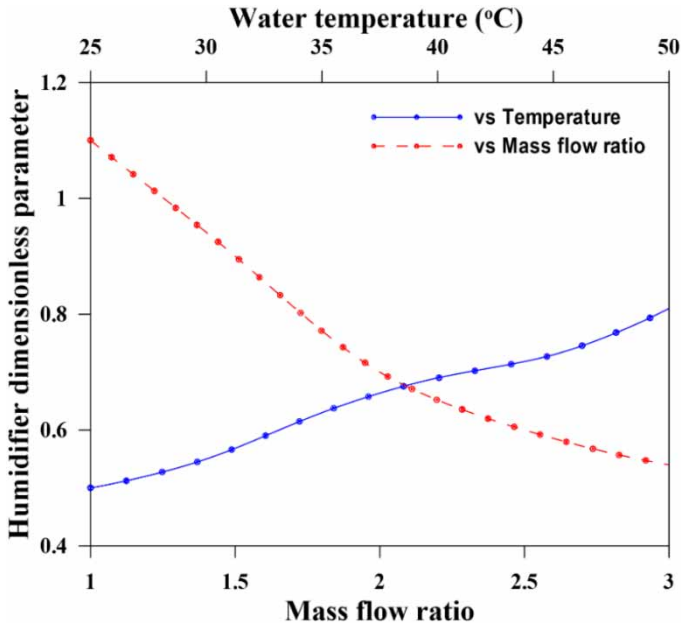

Figure 8 | Dimensionless parameter (kav/M_w) of humidifier vs mass flow ratio.

Table 4 | Summary of cost calculations

Component	Cost in Rs (as per local market)
(a) Calculation of total initial cost (C_T)	
Humidifier	10,000
Dehumidifier	15,000
Air heater	17,000
Water pump	3,000
Fan	2,000
Water tank	9,000
Other	4,000
	Total (C_T) = 60,000 Rs (720 $)
(b) Parameters of economic analysis	
Parameters	**Value**
Plant life (n)	12 years
Interest rate (r)	4, 8, 12%
Average operating and maintenance cost	15% of C_A
Salvage value	15% of C_T
No. of working days	300
(c) Equations used in analysis	
Parameters	**Equation**
Annual cost (C_A)	$C_T \times F_{CR}$
Capital recovery factor (F_{CR})	$r.(1+r)^n / (1+r)^n - 1$
Annual salvage value (C_S)	$SV.\, r/\,(1+r)^n \;-\; 1$
Annual actual total cost (C_{AA})	$C_A + C_M + C_O - C_S$
Cost of water (C_w)	C_{AA}/AY
Payback period	C_T/Total gain

of the analysis is given in Figure 9 which reveals that the average cost of water per kg from HDD-O2 is 0.04 $ and the corresponding payback period is 1.73 years.

Enviro-economic analysis

The HDD-O_2 plant also contributes toward environment safety as the thermal energy demand for yield is provided by SAHJP and waste heat of medical O_2 plants. Therefore, the corresponding reduction in CO_2 emission and enviro-economic cost for HDD-O_2 have been assessed by the relation and corresponding values as suggested by Joshi & Tiwari (2018):

$$\text{Annual } CO_2 \text{ mitigation } (\Phi_{Co2}) = (\psi\,.\,E)/1000, \tag{14}$$

$$\text{enviro} - \text{economic cost } (z_{co2}) = P_{Co2}.\,\Phi_{Co_2} \tag{15}$$

Considering the recommended values of ψ (average CO_2 emission by coal/annum) as 2 kg/kWh and enviro-economic cost (P_{CO_2}) as 14.5 $/t, CO_2 mitigation from the HDD-O_2 unit is 3.2 t/annum, whereas the cost involved is 46.4 $/annum.

Performance comparison

Table 5 compares the performance of the HDD-O_2 unit with the existing systems working on HDD and other methods, on the basis of novelty in method, yield, cost of water, and GOR that are measures of energy efficiency. It is clear that yield and GOR of the HDD-O_2 unit is very attractive compared to the existing units and a novel approach of the HDD-O_2 unit based on waste heat of medical O_2 plants and SAHJP is responsible for the same. Although the cost is higher in comparison to some

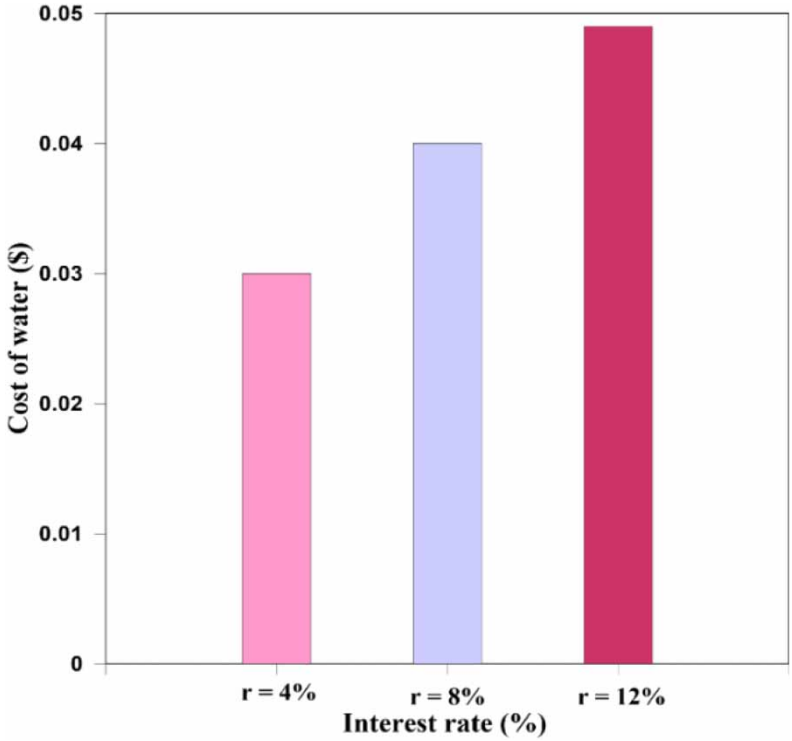

Figure 9 | Cost of water vs interest rate.

Table 5 | Comparison with the existing systems

Reference	Novelty in method	Yield	GOR/Efficiency	Cost
Behnam & Shafii (2016)	Bubble column humidifier, evacuated tube collectors and heat pipes	6.27 kg/d	0.65	0.028 $/L
Abdullah *et al.* (2019)	Drum distiller	9.2 kg/d	0.85	0.039 $/L
Thanaiah *et al.* (2021)	Artificial and bio-based packing materials	0.73 kg/h	0.65	–
Soomro *et al.* (2022)	Hydrophobic packing materials	0.64 kg/h	1.45	–
Shaikh & Ismail (2023)	Multistage bubble column dehumidification	4.57 kg/d	0.79	0.071 $/L
Muftah *et al.* (2023)	Basin-type stepped solar still	6.10 kg/m^2	0.52	0.07 $/L
Tiwari & Kumar (2024)	Double-end open evacuated tube solar air heater	3.12 kg/d/m^2	0.31	0.038 $/kg
Present work	Waste heat of O_2 plants and SAHJP	11 kg/d	1.4	0.04 $/kg

approaches due to additional expenses for the utilization of waste heat, it is still competitive due to the achieved gain in yield and GOR. Overall, Table 5 emphasizes the suitability of HDD-O_2 as an enhancement approach for the HDD process.

CONCLUSIONS

The proposed HDD-O_2 system has been analyzed in this work in comparison with a conventional HDD-C unit. The performance comparison was performed with the help of mathematical simulation. The results and discussion section elaborated on the gain achieved by the HDD-O_2 unit for different operating parameters. The key findings are summarized as follows:

- Hot air from O_2 plants augmented the productivity of the HDD unit.
- The mass flow rate of air in the range 0.03–0.04 kg/s is the most beneficial with the GOR close to 1.2.
- The feeding rate of 0.03 kg/s of brackish water provided a daily yield around 8.1 kg/d.
- The cooling water rate of 0.05 kg/s can raise the yield to around 10 kg/d.

- A high temperature of feed water and a low temperature of cooling water both resulted in a continuous rise in yield and GOR.
- On average, HDD-O_2 resulted in about 43% higher yield compared to HDD-C.
- The cost of water from HDD-O_2 is 0.04 $ and the payback period is 1.73 years.
- The annual CO_2 mitigation from the HDD-O_2 unit is 3.2 t and the enviro-economic cost is 46.4 $/annum.

To further enhance the performance and viability of an HDD-O_2 unit, it is recommended that optimization of the system components can be done, modification can be included to improve the condensation-evaporation process, and CFD simulation can serve to study the flow of the working fluid though the system.

DATA AVAILABILITY STATEMENT

All relevant data are included in the paper or its Supplementary Information.

CONFLICT OF INTEREST

The authors declare there is no conflict.

REFERENCES

Abdel Dayem, A. M. & Al Zahrani, A. (2022) Psychometric study and performance investigation of an efficient evaporative solar HDH water desalination system, *Sustainable Energy Technologies and Assessment*, **52**, 102030. doi:10.1016/j.seta.2022.102030.

Abdullah, A. S., Essa, F. A., Omara, Z. M. & Bek, M. A. (2018) Performance evaluation of a humidification–dehumidification unit integrated with wick solar stills under different operating conditions, *Desalination*, **441**, 52–61. doi:10.1016/j.desal.2018.04.024.

Abdullah, A. S., Essa, F. A., Omara, Z. M., Rashid, Y., Hadj-Taieb, L., Abdelaziz, G. B. & Kabeel, A. E. (2019) Rotating-drum solar still with enhanced evaporation and condensation techniques: Comprehensive study, *Energy Conversion and Management*, **199**, 112024. doi:10.1016/j.enconman.2019.112024.

Abedi, M., Tan, X., Klausner, J. F. & Bénard, A. (2023) Solar desalination chimneys: Investigation on the feasibility of integrating solar chimneys with humidification–dehumidification systems, *Renewable Energy*, **202**, 88–102. doi:10.1016/j.renene.2022.11.069.

Alghassab, M. A. (2024) A review of hybrid solar desalination systems: Structure and performance, *Water Science and Technology*, **89** (5), 1357–1381. doi:10.2166/wst.2024.042.

Alrbai, M., Enizat, J., Hayajneh, H., Qawasmeh, B. & Al-Dahidi, S. (2022) Energy and exergy analysis of a novel humidification-dehumidification desalination system with fogging technique, *Desalination*, **522**, 115421. doi:10.1016/j.desal.2021.115421.

Behnam, P. & Shafii, M. B. (2016) Examination of a solar desalination system equipped with an air bubble column humidifier, evacuated tube collectors and thermosyphon heat pipes, *Desalination*, **397**, 30–37. doi:10.1016/j.desal.2016.06.016.

Chen, Q., Burhan, M., Shahzad, M. W., Ybyraiymkul, D., Akhtar, F. H. & Ng, K. C. (2020) Simultaneous production of cooling and freshwater by an integrated indirect evaporative cooling and humidification-dehumidification desalination cycle, *Energy Conversion and Management*, **221**, 113169. doi:10.1016/j.enconman.2020.113169.

Easa, A. S., Mohamed, S. M., Barakat, W. S., Habba, M., Kandel, M. G. & Khalaf-Allah, R. A. (2023) Water production from a solar desalination system utilizing a high-speed rotary humidifier, *Applied Thermal Engineering*, **224**, 120150. doi:10.1016/j.applthermaleng.2023.120150.

Elminshawy, N. A. S., Siddiqui, F. R. & Addas, M. F. (2016) Development of an active solar humidification-dehumidification (HDH) desalination system integrated with geothermal energy, *Energy Conversion and Management*, **126**, 608–621. doi:10.1016/j.enconman.2016.08.044.

Faizan, M., Toor, Z. & Antar, M. A. (2022) Optimization of two-stage modified air heated HDH desalination systems, *Arabian Journal of Science and Engineering*, **47**, 16451–16473. doi:10.1007/s13369-022-06846-x.

Jabari, F., Nazari-Heris, M., Mohammadi-Ivatloo, B., Asadi, S. & Abapour, M. (2020) A solar dish Stirling engine combined humidification-dehumidification desalination cycle for cleaner production of cool, pure water, and power in hot and humid regions, *Sustainable Energy Technologies and Assessment*, **37**, 100642. doi:10.1016/j.seta.2020.100642.

Joshi, P. & Tiwari, G. N. (2018) Energy matrices, exergo-economic and enviro-economic analysis of an active single slope solar still integrated with a heat exchanger: A comparative study, *Desalination*, **443**, 85–98. doi:10.1016/j.desal.2018.05.012.

Kabeel, A. E., Abdelgaied, M. & Omara, Z. M. (2022) Experimentally evaluation of split air conditioner integrated with humidification-dehumidification desalination unit for better thermal comfort, produce freshwater, and energy saving, *Journal of Thermal Analysis and Calorimetry*, **147**, 4197–4207.

Khass, T. M., Mohammed, R. H., Qasem, N. A. A. & Zubair, S. M. (2022) Different configurations of humidification-dehumidification desalination systems: Thermal and economic assessment, *Energy Conversion and Management*, **258**, 115470. doi:10.1016/j.enconman.2022.115470.

Lawal, D., Antar, M., Khalifa, A., Zubair, S. & Al-Sulaiman, F. (2018) Humidification-dehumidification desalination system operated by a heat pump, *Energy Conversion and Management*, **161**, 128–140. doi:10.1016/j.enconman.2018.01.067.

Matheswaran, M. M., Arjunan, T. V. & Somasundaram, D. (2018) Analytical investigation of solar air heater with jet impingement using energy and exergy analysis, *Solar Energy*, **161**, 25–37. doi:10.1016/j.solener.2017.12.036.

Moshery, R., Chai, T. Y., Sopian, K., Fudholi, A. & Al-Waeli, A. H. A. (2021) Thermal performance of jet-impingement solar air heater with transverse ribs absorber plate, *Solar Energy*, **214**, 355–366. doi:10.1016/j.solener.2020.11.059.

Muftah, A. F., Sopian, K., Ibrahim, A., Elbreki, A. & Abed, A. M. (2023) Design and evaluation of a modified basin-type stepped solar-still under Malaysia climate conditions, *Energy Sources, Part A: Recovery, Utilization, and Environmental Effects*, **45**, 6756–6771. doi:10.1080/15567036.2023.2216177.

Qasem, N. A. A., Zubair, S. M., Abdallah, A. M., Elbassoussi, M. H. & Ahmed, M. A. (2020) Novel and efficient integration of a humidification-dehumidification desalination system with an absorption refrigeration system, *Applied Energy*, **263**, 114659. doi:10.1016/j.apenergy.2020.114659.

Sachdev, T., Gaba, V. K. & Tiwari, A. K. (2020) Performance analysis of desalination system working on humidification-dehumidification coupled with solar assisted air heater and wind tower: Closed and open water cycle, *Solar Energy*, **205**, 254–262. doi:10.1016/j.solener.2020.04.083.

Santosh, R., Yoo, C. H. & Kim, Y. D. (2022) Performance evaluation and optimization of humidification–dehumidification desalination system for low-grade waste heat energy applications, *Desalination*, **526**, 115516. doi:10.1016/j.desal.2021.115516.

Shaikh, J. S. & Ismail, S. (2023) Performance evaluation of a solar humidification dehumidification desalination system employing a multistage bubble column dehumidifier, *Solar Energy*, **263**, 111933. doi:10.1016/j.solener.2023.111933.

Shamet, O., Lawal, D. U., Al Hariri, A. H. & Antar, M. (2023) Performance of different HDH desalination units powered by diesel engine generator waste heat, *Process Safety and Environmental Protection*, **179**, 651–666. doi:10.1016/j.psep.2023.09.046.

Shojaei, M., Mortezapour, H. & Jafarinaeimi, K. (2020) Experimental investigation of a heat pump-assisted solar humidification–dehumidification desalination system with a free-flow solar humidifier, *International Journal of Environmental Science and Technology*, **17**, 2401–2414. doi:10.1007/s13762-019-02554-6.

Soomro, S. H., Santosh, R., Bak, C., Yoo, C., Kim, W. & Kim, Y. (2022) Effect of humidifier characteristics on performance of a small-scale humidification-dehumidification desalination system, *Applied Thermal Engineering*, **210**, 118400. doi:10.1016/j.applthermaleng.2022.118400.

Sun, Z., Tu, W., Fang, S. & Zhong, W. (2022) Comparison between double slope solar still and fourfold slope solar still: Energy, exergy, exergoeconomic, and enviroeconomic evaluation, *Water Supply*, **22** (3), 2929–2945. doi:10.2166/ws.2021.425.

Thanaiah, K., Gumtapure, V. & Tadesse, G. M. (2021) Experimental analysis on humidification-dehumidification desalination system using different packing materials with baffle plates, *Thermal Science and Engineering Progress*, **22**, 100831. doi:10.1016/j.tsep.2020.100831.

Tiwari, A. & Kumar, A. (2024) Energy, exergy, economic, exergo and enviro-economic analysis of solar powered humidification dehumidification desalination system: An experimental investigation, *Applied Thermal Engineering*, **246**, 122992. doi:10.1016/j.applthermaleng.2024.122992.

Welepe, H. J. N., Günerhan, H. & Bilir, L. (2022) Humidifying solar collector for improving the performance of direct solar desalination systems: A theoretical approach, *Applied Thermal Engineering*, **216**, 119043. doi:10.1016/j.applthermaleng.2022.119043.

Yamali, I. C. & Solmus, I. (2006) Theoretical investigation of a humidification-dehumidification desalination system configured by a double-pass flat plate solar air heater, *Desalination*, **205**, 163–177.

Zarei, T. & Adibi, P. (2023) Operational analysis of a humidification–dehumidification desalination in packed bed humidifier and dehumidifier columns with salt- and freshwater recirculation, *Journal of Brazilian Society of Mechanical Sciences and Engineering*, **45**, 635. doi:10.1007/s40430-023-04556-5.

First received 5 May 2024; accepted in revised form 21 July 2024. Available online 19 September 2024